Upper critical fields and reduced dimensionality of the superconducting layered compounds

D. E. Prober
Department of Engineering and Applied Science, Becton Center, Yale University, New Haven, Connecticut 06520

R. E. Schwall*
Department of Applied Physics, Stanford University, Stanford, California 94305

M. R. Beasley
Departments of Applied Physics and Electrical Engineering, Stanford University, Stanford, California 94305

(Received 10 February 1978; revised manuscript received 18 September 1979)

A detailed study of the critical magnetic fields of the superconducting layered compounds is reported and used to investigate the quasi-two-dimensional nature of these superconductors. The compounds studied include TaS_2 and $TaS_{1.6}Se_{0.4}$ intercalated with collidine, pyridine, or aniline and the unintercalated compounds $TaS_{1.6}Se_{0.4}$ and $NbSe_2$. The parallel critical fields of the intercalated compounds are found to be extremely high, rising faster with decreasing temperature (up to 200 kOe/K in the case of the $TaS_{1.6}Se_{0.4}$ intercalation complexes) than for any other known superconductor. Ginzburg-Landau coherence lengths derived from the data indicate that the intercalated compounds should behave two dimensionally at low temperatures. It is found that the critical-field behavior is in qualitative agreement with the theoretical predictions of Klemm, Beasley, and Luther, based on the model of layered compounds as two-dimensional superconducting layers weakly coupled via Josephson tunneling. However, not all features of the data can be explained by this model. In addition, it is found that the observed critical fields are too high to be consistent with the conventional theory of Pauli paramagnetic limiting of the critical fields in superconductors.

I. INTRODUCTION

Following the discovery[1] of superconductivity in layered transition-metal dichalcogenides intercalated with organic molecules, a number of fundamental questions have arisen regarding the nature of the superconductivity in these compounds and the effect on their superconducting properties of the quasi-two-dimensional character of these materials.[2,3] Initially the greatest interest revolved around the finding by Gamble *et al.*[1] that intercalation of organic molecules into the layered compounds could increase the transition temperature T_c of the material dramatically, possibly suggesting a novel mechanism for the superconductivity.[3] It is now generally agreed, however, that the observed increase in T_c results from suppression of charge-density wave formation in these compounds[4] rather than some exotic mechanism of superconductivity or even quasi-two dimensionality per se.[3] The effects of quasi-two dimensionality on the other superconducting properties of these materials remain, however, of considerable interest.

In an earlier study[5] we have shown that, in the particular case of TaS_2 (pyridine)$_{1/2}$, the fluctuation superconductivity just above T_c is three dimensional in nature, contrary to earlier speculation. Two-dimensional fluctuations are expected well above T_c where the layers decouple, but according to theory[6] this regime is beyond the temperature range within which reliable measurements could be made at that time. On the other hand, the quasi-two-dimensional nature of these materials is expected to manifest itself directly in the behavior of the upper critical field, H_{c2}. In fact, H_{c2} has been predicted[6] to exhibit rather unusual behavior (including a kind of dimensional-crossover phenomenon) on the basis of the two-dimensional, Josephson-coupled superconductor model originally introduced by Lawrence and Doniach.[7]

In order to explore this possibility and to attempt to understand the extremely large critical fields exhibited by the intercalated layered compound superconductors, we have undertaken an extensive study of the upper critical fields of a series of intercalation complexes of TaS_2 and $TaS_{1.6}Se_{0.4}$. For comparison the unintercalated compounds $TaS_{1.6}Se_{0.4}$ and $NbSe_2$ have also been studied, but to a much lesser extent.

Experimental studies of the critical fields of unintercalated layered compound superconductors have been reported previously by various researchers. The material most extensively studied[8,9] is the unintercalated metal $NbSe_2$. This compound has the highest superconducting transition temperature of all the layered compounds ($T_c = 7.1$ K) but only a moderate critical-field anisotropy (approximately a factor of 3 between applied fields parallel and perpendicular to

the layers.) Somewhat larger anisotropies, but qualitatively similar behavior, are seen for the layered compounds of MoS_1 intercalated with alkali and alkaline-earth metals.[10]

Studies of the critical fields of organic-intercalated compounds have been made by Foner *et al.*,[11] Morris and Coleman,[12] Schwall *et al.*,[13] and Muto *et al.*[14] These studies, along with the more extensive results reported here, show that the organic intercalation complexes have both much larger critical-field anisotropies than the unintercalated compounds and also extremely large critical fields parallel to the layers (see Fig. 1) $H_{c2\parallel}$, rising faster with decreasing temperature than any other known superconductor. Moreover, the values of $H_{c2\parallel}$ for these intercalated compounds considerably exceed the so-called Pauli paramagnetic limiting field, $H_p = \Delta_0/(\sqrt{2}\mu_B) = 18.6 T_c(\text{kOe})$, resulting from the Pauli paramagnetism of the conduction electrons.[15]

The present work covers a much broader range of intercalated compounds and undertakes far more thorough measurements and interpretation than has been attempted previously. Specifically, H_{c2} has been measured as a function of temperature and orientation for $TaS_2(\text{collidine})_{1/6}$, $TaS_2(\text{pyridine})_{1/2}$, $TaS_2(\text{aniline})_{3/4}$, $TaS_{1.6}Se_{0.4}(\text{collidine})_{1/6}$, $TaS_{1.6}Se_{0.4}(\text{pyridine})_{1/2}$, and the unintercalated compounds $TaS_{1.6}Se_{0.4}$ and $NbSe_2$. From our measured values of $H_{c2}(T)$, we determine the Ginzburg-Landau coherence lengths and other superconducting parameters for these materials and use this information to establish the extent of their reduced dimensionality. The data are also compared with the predictions of the two-dimensional, Josephson-coupled model of the layered superconductors as worked out by Klemm, Beasley, and Luther (KBL).[6]

We find that several of these materials should be quite two dimensional in their superconducting properties at low temperatures, and that the KBL theory accounts rather well for the systematics of the observed critical-field behavior within the class of intercalated compounds taken as a whole. Certain features of the critical-field results, in particular an anomalous curvature in $H_{c2}(T)$ near T_c and the linearity of $H_{c2\perp}(T)$ observed at low temperatures, are not explained by this theory. Also, on the basis of the conventional theory of Pauli paramagnetic pair breaking, very large spin-orbit scattering rates are required to account for the absence of Pauli limiting in the materials at high fields, and these spin-orbit scattering rates are comparable to or larger than the estimated *total* scattering rates. Some new elements to the theory thus appear to be required.

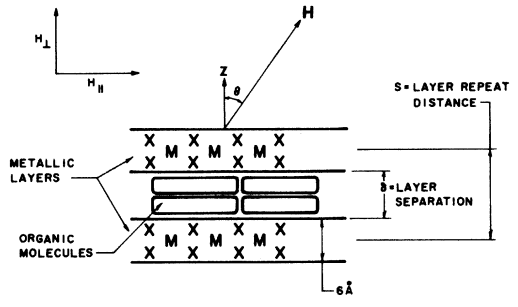

FIG. 1. Schematic of the structure of the intercalated layered compounds, and the definition of field orientations used in this paper. M represents the transition-metal atoms, Ta, or Nb and X the chalcogenide atoms, S or Se.

This paper is organized as follows. In Sec. II we discuss the relevant theoretical calculations of the critical fields of superconductors appropriate to the layered compounds. In Sec. III we discuss sample preparation, the experimental techniques, and the procedures used to analyze the data from such unusual and difficult materials. The critical-field results are presented in Sec. IV. The results are discussed and compared with theory in Sec. V. Conclusions are presented in Sec. VI.

II. THEORETICAL CONSIDERATIONS

Before presenting our experimental results we briefly review the available theories of the critical fields in layered superconductors. This review is intended to provide a general framework for interpreting the data and also to give the reader a physical picture of the results of the more formal theoretical calculations. Although the results of microscopic theory are required for comparison with experiment, we begin with the phenomenological Lawrence-Doniach theory because of its simplicity and because of the physical insight it provides into the results of the microscopic theories.

A. The Lawrence-Doniach theory

In the Josephson-coupled model introduced by Lawrence and Doniach (LD),[7] layered compounds are pictured as a stacked array of two-dimensional superconducting layers which are weakly coupled via Josephson tunneling between adjacent layers. It is essentially the Ginzburg-Landau (GL) theory of a set of weakly coupled two-dimensional superconductors. This model has proved to be a useful starting point for describing the properties of layered compound superconductors.

As shown by Lawrence and Doniach, as $T \to T_c$ the superconducting order parameter varies slowly on the scale of the layer repeat distance, and their theory reduces to the familiar anisotropic Ginzburg-Landau theory.[16] In this theory the pair motion is described in terms of an effective-mass tensor in which the pair

mass for propagation within the layers, m, differs from the mass for motion in the z direction normal to the layers M. In terms of the parameters of the LD theory

$$M = \hbar^2/2s^2\eta \ , \tag{1}$$

where s is the layer repeat distance (see Fig. 1) and η is an interlayer coupling parameter. Thus, M is inversely proportional to the coupling strength η, and we expect that $M >> m$ for weak interlayer coupling.

Within the anisotropic GL theory the critical field is given by

$$H_{c2\theta}(T) = \frac{\Phi_0}{2\pi\xi^2(T)[\cos^2\theta + (m/M)\sin^2\theta]^{1/2}} \ , \tag{2}$$

where $\Phi_0 = hc/2e$ is the flux quantum, and $\xi(T)$ is the GL coherence length within a layer. Further, in the anisotropic GL theory

$$\xi_z^2(T) = (m/M)\xi^2(T) \ , \tag{3}$$

with $\xi_z(T)$ the coherence length perpendicular to the layers. The coherence length describes the length scale over which variations of the order parameter normal to the layer may take place. From Eq. (2) we may determine the mass ratio M/m experimentally as

$$\frac{M}{m} = \left(\frac{H_{c2\parallel}}{H_{c2\perp}}\right)^2 \ . \tag{4}$$

An important consequence of the reduction of the LD theory to the anisotropic GL theory as $T \to T_c$ is that all superconducting properties of layered compounds are expected to be three-dimensional in nature sufficiently near T_c, despite the layered structure of the material. Physically this arises because near T_c the order parameter varies slowly on the scale of the layer repeat distance s and therefore effectively averages over the finer-scale layered structure. For the more weakly coupled intercalated compounds, $\xi_z(T)$ defined by Eq. (3) can be smaller than s, and calculations based on the full LD theory must be considered. Also, at low temperatures, where the GL and LD theories are no longer valid, microscopic theory is required. These calculations are discussed below.

B. Results of the full Lawrence-Doniach theory

Calculations of $H_{c2}(T)$ have been carried out by several researchers[6,17] with the full LD theory. For all field orientations except near parallel, the critical-field curves are essentially those predicted from the anisotropic GL model. With the field oriented parallel to the layers, though, the LD theory predicts very unusual new features for $H_{c2}(T)$ which are a consequence of the layered structure of the materials.

For H parallel to the layers, the LD equation can be reduced to the Mathieu equation, and $H_{c2\parallel}$ is determined from the relation

$$\mathcal{E}(H) = (4/\pi)k_B(T_c - T) \ , \tag{5}$$

where k_B is Boltzmann's constant and $\mathcal{E}$ is the lowest eigenvalue of the equation[6]

$$\left(\frac{8m\xi^2(0)k_BT_c}{\pi\hbar^2}\right)\left(-\frac{\hbar^2}{2m}\frac{d^2}{dx^2} + \frac{\hbar^2}{Ms^2}[1-\cos(2\pi Hxs/\Phi_0)]\right)\Psi = \mathcal{E}\Psi \ . \tag{6}$$

For small fields (i.e., near T_c) this equation reduces to the anisotropic GL theory, as expected. For large fields (i.e., lower temperatures) it predicts a divergence to infinity of $H_{c2\parallel}(T)$ at a temperature T^* defined by the relation

$$\xi_z(T^*) = s/\sqrt{2} \ . \tag{7}$$

The divergence predicted for H_{c2} at T^* is most unusual. It can be interpreted[6] as an indication that at low enough temperatures, $T \leq T^*$, the normal cores of the vortices, which are ellipsoidal in an anisotropic type-II superconductor, have shrunk sufficiently to be able to "fit" in between the superconducting layers and thus no longer affect H_{c2}. This result also suggests that at lower temperatures layered-compound superconductors which are sufficiently weakly coupled should have properties similar to a series array of coupled Josephson junctions. From this point of view the divergence at T^* corresponds to the transition from Abrikosov-like vortices to Josephson-like vortices, in which the normal core has shrunk to a point.

The LD model neglects any effect of the magnetic field on the superconductivity within the individual layers, and this is what allows the unphysical divergence at T^*. To remove this divergence, the effects of Pauli paramagnetism within the layers, as modified by spin-orbit scattering, have been considered in the calculations based on microscopic theory. These are described below. The finite thickness of the layer is not considered because the layers are too thin for this to be a factor in limiting $H_{c2\parallel}$.

C. Microscopic theories

Microscopic theories of the upper critical field relevant to the superconducting layered compounds have been developed from various points of view. One approach has been to adapt the general theory of the critical fields of anisotropic superconductors to

the case of layered compounds.[18] These calculations assume both the energy gap and the Fermi surface are anisotropic, and calculate H_{c2} using the Gor'kov formalism. This is a very complicated approach in general and even relatively simple results are obtained only in the limit of weak anisotropy. This approach is therefore presumably most useful for the unintercalated layered compounds. The effects of Pauli paramagnetism have not yet been included.

Another approach has been to develop the coupled two-dimensional superconductor model starting from microscopic theory and to use this theory to calculate H_{c2}. This approach has been developed independently by Klemm, Beasley, and Luther[6] and by Bulaevskii[19] in various limits. Because these theories presuppose very strong anisotropy, they are presumably more appropriate for the intercalated superconducting layered compounds. These theories also provide a microscopic justification for the LD model and establish the relationship between the phenomenological parameters of that theory (e.g., η) and the microscopic properties of the material. The effects of Pauli paramagnetic limiting and the influence of spin-orbit scattering on the Pauli limiting field are readily incorporated in these models. The limits treated by KBL seem to apply best to our materials and therefore are discussed here in detail. Bulaevskii's results are for the limit of negligible interlayer coupling, and weak spin-orbit scattering, and cannot be directly applied for the materials studied here.

The KBL calculations of $H_{c2\parallel}(T)$ for layered compounds have been carried out using the microscopic Gor'kov theory in the dirty limit, i.e., in the limit where $l \ll \xi_0$, with l being the electron mean free path within the layer, and ξ_0 the BCS coherence length, also within the layer. Also, the KBL theory is for the case in which the electrons scatter many times within a given layer before tunneling to the next layer. The result for $H_{c2\perp}(T)$ is the same as that predicted for conventional dirty type-II superconductors.[20] Near T_c it reduces to the LD result.

The results for $H_{c2\parallel}(T)$ have been calculated in the limit of $\tau_{so}\mu_B H/\hbar \ll 1$, where τ_{so} is the spin-orbit scattering time. It this limit, the KBL calculation reduces to the usual pair-breaking equation for a dirty type-II superconductor

$$\ln\left(\frac{T}{T_c}\right)+\psi\left(\frac{1}{2}+\frac{\rho}{2\pi k_B T}\right)-\psi\left(\tfrac{1}{2}\right)=0 \quad , \tag{8}$$

where $\psi(z)$ is the digamma function, and the pair-breaking parameter ρ is given by

$$\rho=\mathcal{E}(H)+3\tau_{so}(\mu_B H)^2/2\hbar \quad , \tag{9}$$

with $\mathcal{E}$ given by Eq. (5). As in the conventional theory, pair breaking is due to both the orbital motion of the pairs (i.e., the vortices) and to Pauli paramagnetic limiting. The new physics for the layered compounds is contained in the unusual field dependence of $\mathcal{E}$ (see Ref. 6) associated with the layered nature of the superconductor.

The theory employs a number of parameters that are relevant to the data analysis given in Sec. V. These are

$$\alpha \equiv \frac{\Phi_0/2\pi\xi(0)\xi_z(0)}{4k_B T_c/\pi\mu_B}=\frac{dH_{c2\parallel}/dT}{18.95(kG/K)} \quad , \tag{10}$$

which characterizes the relative strength of pair breaking due to Pauli paramagnetism (assuming no spin-orbit scattering) compared to that due to orbital effects, and the parameter

$$r=\frac{4}{\pi}\left(\frac{\xi_z(0)}{\frac{1}{2}s}\right)^2 \quad , \tag{11}$$

which characterizes the relative two dimensionality of the material. Smaller r values indicate a greater degree of two dimensionality.

Curves for $H_{c2\parallel}(T)$ have been calculated by KBL for a range of values of these parameters and spin-orbit scattering times. The normalized spin-orbit scattering time, $\tau_{so}T_c$, is related[20] to the spin-orbit scattering parameter λ_{so} employed by Werthamer and co-workers by

$$\tau_{so}T_c=2/3\pi\lambda_{so}=2l_{so}/3\pi(1.17\xi_0) \quad , \tag{12}$$

where l_{so} is the electron mean free path for spin-orbit scattering. (For this and similar equations, $\hbar=k=1$.) The curves for $\tau_{so}T_c=0$ calculated by KBL have exactly the same divergent behavior as that predicted by the LD theory, since for $\tau_{so}T_c=0$, Pauli paramagnetism has no effect in limiting $H_{c2\parallel}$. For the microscopic theory, this divergence occurs near but just below T^*, the temperature at which the LD result diverges.

This divergence or upturn of $H_{c2\parallel}(T)$ is in fact a signature of a dimensional-crossover effect, where near T_c the material behaves like an anisotropic three-dimensional superconductor, while at low temperatures the behavior is determined essentially by the properties of the individual layers acting as a series array of Josephson junctions. This crossover is seen clearly in Fig. 2 for the curves with $r=1$. (For all curves in the figure $\alpha=1$ and $\tau_{so}T_c=0.015$.) As is evident in the figure, the width of the three-dimensional region near $T_c[H_{c2\parallel}(T)\propto(T_c-T)]$ is determined by the strength of the interlayer coupling, becoming vanishingly small as $r\to 0$. In this limit $H_{c2\parallel}(T)$ approaches the result for a pure Pauli paramagnetically limited superconductor, for which $H_{c2}(T)\propto(T_c-T)^{1/2}$. At the other extreme, the curve for $r=10$ is essentially identical to the usual result for three-dimensional type-II superconductors.

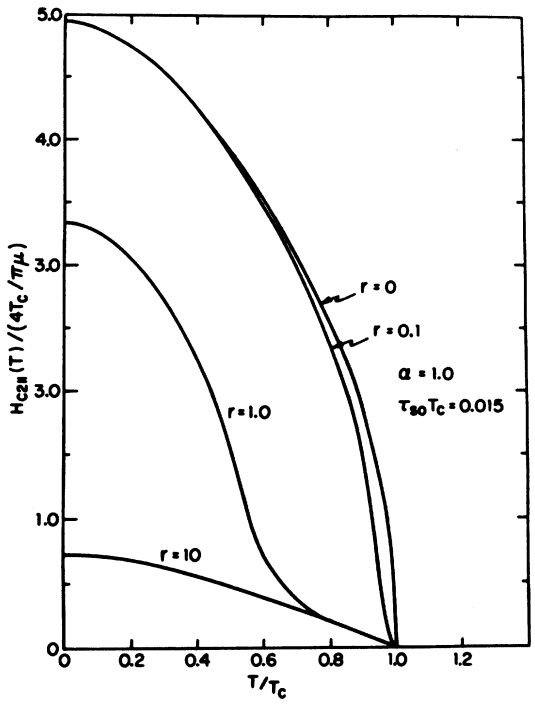

FIG. 2. Parallel critical fields predicted by KBL theory for various interlayer coupling strengths $r = 16\xi_z^2(0)/\pi s^2$. Curve for $r = 1$ shows upturn predicted by the LD result, and is indicative of the dimensional crossover effect. Curve for $r \to 0$ corresponds to Pauli limiting field in a very thin film (from Klemm *et al.*, Ref. 6).

Although in this figure $\tau_{so}T_c$ is not varied, KBL's results show that the dramatic upturn for $r = 1$ is evident only for very small values of $\tau_{so}T_c$. Thus, the dimensional-crossover effect will not always result in such an upturn of $H_{c2\parallel}$; this is relevant in our discussions later.

A related dimensional-crossover phenomenon is also expected[5] in the superconducting fluctuation effects above T_c. In this case a three-dimensional region just above T_c is predicted, with two-dimensional effects expected well above T_c. For the compounds whose fluctuation have been studied to date, only the three-dimensional region has been experimentally accessible and the two-dimensional region has not been seen in the fluctuation studies.

In summary, the KBL results show that for $T \approx T_c$, $H_{c2\parallel}$ is determined largely by the orbital pair-breaking characteristic of bulk superconductors, and is linear in $(T_c - T)$. For $T < T^*$, $H_{c2\parallel}$ is determined largely by the destruction of the superconductivity within the individual layers. This crossover from anisotropic type-II behavior near T_c to individual-layer behavior at lower temperatures is apparent in the H_{c2} curves, however, only for very small values of $\tau_{so}T_c$.

III. SAMPLE PREPARATION, EXPERIMENTAL METHODS AND DETERMINATION OF H_{c2}

A. Sample preparation and characteristics

The samples studied were as-grown single-crystal flakes, with typical dimensions $\sim 3 \times 3 \times 0.2$ mm^3. Most of the crystals used were synthesized at Stanford University by one of us (R.E.S.). Some TaS_2 intercalation complexes supplied by Dr. A. H. Thompson of Exxon were also investigated.

The preparation and structural properties have already been reported[1,21–23] in detail for the TaS_2 compounds and $NbSe_2$, and for the $TaS_{1.6}Se_{0.4}$ compounds.[24] Briefly, the growth procedure is the following. A powder of the unintercalated metal (e.g., TaS_2) is first grown by reacting the components at a

TABLE I. Sample parameters. *s*-collidine = $(CH_3)_3C_5H_2N$, pyridine = C_5H_5N, aniline = $C_6H_5NH_2$.

	T_c (K)	ΔT_c (K) (0.1 → 0.9 transition width)	δ = Layer repeat distance (Å)	Stacking polytype	Comments
TaS_2(collidine)$_{1/6}$	3.2	0.2	9.7[a]	2*H*	Some wrinkling of crystals
TaS_2(pyridine)$_{1/2}$[b]	3.47	0.2	12.0[a]	2*H*	Some wrinkling; 2 samples measured in high fields
TaS_2(aniline)$_{3/4}$	2.9	0.2	18.1[a]	2*H*	Some wrinkling; 2 samples measured in high fields; small crystals
$TaS_{1.6}Se_{0.4}$	4.1	0.07	6.1[c]	4*H*	Measured only to 12 kG
$TaS_{1.6}Se_{0.4}$(collidine)$_{1/6}$	2.6	0.19	9.7[c]	4*H*	
$TaS_{1.6}Se_{0.4}$(pyridine)$_{1/2}$	2.1	0.13	12.1[c]	4*H*	
$NbSe_2$	7.1	0.07	6.3[d]	2*H*	Measured only to 12 kG

[a]See Ref. 1.
[b]For TaS_2(pyridine)$_{1/2}$ excess sulfur was dissolved in the pyridine liquid (see text).
[c]See Ref. 22.
[d]See Ref. 25.

temperature of 700–1000 °C in a sealed quartz tube. Single crystals are then grown by iodine-vapor transport. To intercalate the samples the single crystals are sealed with an excess of the organic intercalant in a quartz tube, and reacted at 150–200 °C for between one and four weeks. The detailed preparation procedures followed for our samples, using TaS_2(pyridine)$_{1/2}$ as an example, have already been summarized by us previously.[5] A list of the samples studied and some of their material parameters is given in Table I.

The samples used in this study were generally of good quality as judged from the relatively narrow zero-field transitions and the reproducibility of their material properties. The most difficult problem encountered in our critical-field studies is that the intercalated TaS_2 crystals are slightly wrinkled. This complicates measurement of the angular dependence of H_{c2} but not the strictly parallel value $H_{c2\parallel}$ as we shall see. The wrinkling appears to be present even in the unintercalated crystals, and is believed to be caused by strains resulting from a change in the volume of the unit cell during cooling from the high-temperature $1T$ polytype, in which the crystal grows, to the superconducting $2H$ polytype, which is stable at low temperatures. Smaller TaS_2 crystals would presumably be less wrinkled. The $TaS_{1.6}Se_{0.4}$ crystals on the other hand appear to be free of wrinkling, although some twinning of the crystals is observed. Another potential complication in the particular case of TaS_2(pyridine)$_{1/2}$ is that two molecular stacking arrangements of the pyridine are possible: one with a layer separation of $\delta = 5.85$ Å, the other with $\delta = 6.01$ Å. In our measurements we have used only single-phase TaS_2(pyridine)$_{1/2}$ with $\delta = 6.01$ Å. Such single-phase compounds are obtained by intercalating with pyridine containing dissolved sulfur.[25]

B. Experimental methods

Data for $H_{c2}(T)$ were determined primarily from measurements of the ac magnetic susceptibility of individual single-crystal samples with a mutual inductance circuit. In some cases H_{c2} was also determined from the resistive transition.

Measurements for perpendicular and parallel field orientations were carried out for all compounds listed in Table I, and for intermediate angles in a few representative cases. Two samples each of TaS_2(pyridine)$_{1/2}$ and TaS_2(aniline)$_{3/4}$, and one sample each of TaS_2(collidine)$_{1/6}$, $TaS_{1.6}Se_{0.4}$(pyridine)$_{1/2}$, and $TaS_{1.6}Se_{0.4}$(collidine)$_{1/6}$ were run in high fields (to 120 kOe). These were selected from a much larger number of samples run in low fields, and had the narrowest zero-field and parallel-field transitions. $NbSe_2$ and $TaS_{1.6}Se_{0.4}$ samples were run only in low fields to determine their behavior near T_c.

Our choice of the ac susceptibility technique was made in order to allow rapid acquisition of data for even very small samples. Measurements were made on samples as small as $1 \times 1 \times 0.1$ mm^3. In addition, as discussed below, we find that the properties measured with the ac susceptibility technique appear to be representative of bulk crystal properties.

To carry out these measurements, two cryostats were constructed. One was used in a low-field iron-core magnet, with a maximum field of 12 kG. This cryostat was used to survey a large number of samples, to select candidates for study in high fields and also to provide information on reproducibility of T_c and the critical fields. The second cryostat was used with a high-field superconducting Nb_3Sn solenoid, having a maximum field of approximately 120 kG, with a clear bore of 1.46 in. The cryostats were constructed on the same principles. The major difference in design is that in the high-field cryostat, the sample and the coils surrounding it are rotated inside the bore of the superconducting solenoid, using a bevel gear drive with a control rod from outside the Dewar. This is shown in Fig. 3. In the low-field cryostat, the magnet is rotated outside the Dewar. Note that in both cases the circulating ac currents flow in the plane of the layers, and only the angle between the sample and the applied dc field is varied. Measurements were made mostly at 100 kHz, with a few measurements at 5 kHz. The amplitude of the applied ac field ranged from 4 to 40 mG, and the measured transitions were found to be amplitude independent.

The samples in the form of single-crystal flakes were glued onto the flat end of a single-crystal sapphire rod with GE 7031 cement. The sapphire rod

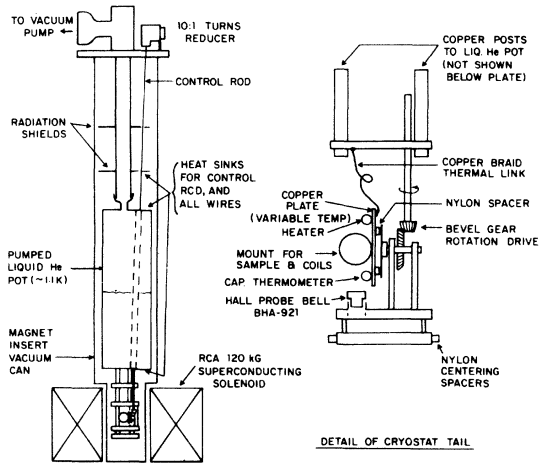

FIG. 3. Schematic diagram of the high-field ac susceptibility cryostat. The sample mount holds a sapphire rod onto which the sample is glued. Nylon spacers isolate the variable-temperature copper plate from the bevel gear drive, which is held at 1.1 K.

holds the sample in the pickup coil, with the face normal of the sample parallel to the axis of the coil. The sapphire rod is clamped to a copper stirrup on a variable-temperature copper plate (see Fig. 3). A layer of Apiezon N-grease was used to ensure good thermal contact. The copper plate is supported by nylon screws, and is weakly linked to the bath by a copper braid. It rotates inside the magnet bore, driven by a bevel gear arrangement. Also on this copper plate are mounted a germanium resistance thermometer, a capacitance thermometer[26] (Lake Shore Cryotronics CS-400GR) and a metal-film heater resistor. The magnetic field of the superconducting solenoid is measured with a doped GaAs Hall Probe, F. W. Bell BHA-921, mounted near the sample. This probe was calibrated in the iron-core magnet at 4.2 K against the Varian Fieldial controller.

During data taking the capacitance thermometer was used because its characteristics are unaffected by large magnetic fields. However, its characteristics can shift by up to 0.1 K after cycling to room temperature,[27] so the resistance thermometer was used to check the calibration of the capacitance thermometer in low fields each day. The small day-to-day shifts in the characteristics of the capacitance thermometer were compensated by suitable adjustments of the bridge circuit used to measure the capacitance. This bridge circuit is described in detail elsewhere.[27] Other than the need to reset the capacitance thermometer for each day's run, operation of either cryostat was quite reliable and routine.

In operation the sample temperature is swept in a fixed magnetic field since this minimizes helium losses as compared with a swept-field measurement. Also, the observed background effects and drifts are far more field dependent than temperature dependent. The two different types of sweeps yield the same transition fields, however.

For a small number of samples, simultaneous measurements of ac resistive and ac susceptibility transitions were made in low fields. Resistance, defined as $V(\omega)/I(\omega)$, was measured with separate pairs of current and voltage leads attached with conducting silver paint to the exposed fact of the mounted sample. ac currents of 1 mA were used, at a frequency of 1 kHz. Assuming uniform current flow, current densities were 0.1–1 A/cm^2.

C. Determination of H_{c2}

Typical ac susceptibility data are shown in Fig. 4 for various perpendicular dc fields. We use TaS_2(pyridine)$_{1/2}$ as an example. As seen in the figure, the ac magnetic field is fully shielded from the sample volume at low temperatures. These curves are reversible for the most part, although for $NbSe_2$ a small amount of hysteresis on temperature cycling is evident at lower temperatures. The determination of

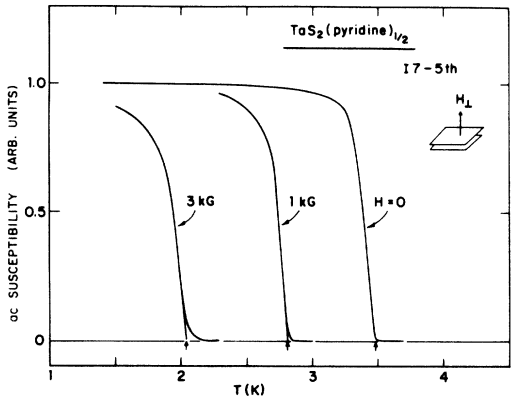

FIG. 4. ac susceptibility transitions for TaS_2(pyridine)$_{1/2}$ in perpendicular applied fields. The identification of $T_{c2}(H)$ is indicated by arrows. Measurement frequency is 100 kHz.

$H_{c2}(T)$ [or $T_{c2}(H)$ in our experiments] from ac susceptibility data requires the selection of some characteristic point on the transition curve as H_{c2}. The aim here is to find a procedure for determining H_{c2} which is both self-consistent and which yields H_{c2} values in accord with available data obtained by other measurement techniques.

Our identification of $T_{c2}(H)$ in Fig. 4 is indicated by small arrows. So defined, $T_{c2}(H)$ corresponds to the highest temperature to which shielding of the ac field persists. The values of $T_{c2}(H_\perp)$ which result from this analysis are in good agreement with those derived from measurements of specific heat in a field[13] on samples from the same TaS_2(pyridine)$_{1/2}$ intercalation batch, *I*7. Similar agreement is found for our measurements on $NbSe_2$, $TaS_{1.6}Se_{0.4}$, and $TaS_{1.6}Se_{0.4}$(pryidine)$_{1/2}$.

This procedure identifying T_{c2} is quite straightforward for the perpendicular field orientation, since the shape of the transition remains constant as the field increases. Data for H parallel to the layers, on the other hand, are more complicated. Typical parallel field transitions are shown in Fig. 5 for the same TaS_2(pyridine)$_{1/2}$ crystal shown in Fig. 4. In large parallel fields, the transitions are significantly broadened (width proportional to H), and identification of $T_{c2}(H)$ is more difficult. This broadening in high fields most likely results from these regions in the sample whose crystallographic alignment with respect to the applied dc field is not quite parallel. Resistance measurements (see below) in fact show that to some extent misalignments as large as 90° do occur even in the best crystals. We have therefore used the extrapolation procedure illustrated in Fig. 5 for the parallel field direction, as this procedure emphasizes the highest-temperature part of the curves corresponding to those regions of the sample which are aligned exactly parallel to the dc field. While such a procedure should compensate for misoriented

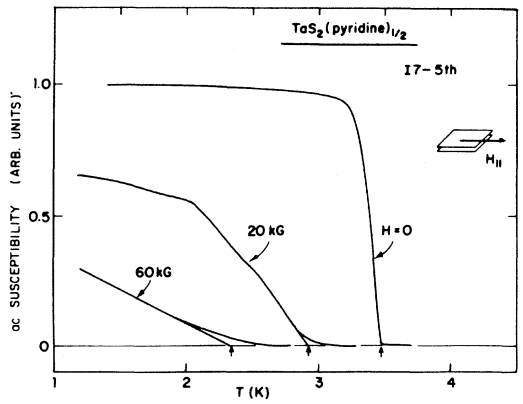

FIG. 5. ac susceptibility transition for $TaS_2(pyridine)_{1/2}$ in parallel applied fields. The identification of $T_{c2}(H)$ is indicated by arrows. Measurement frequency is 100 kHz. The significant broadening seen is believed to be due to misoriented regions within the sample. Rationale for choice of T_{c2} discussed in text.

regions, we expect the resulting H_{c2} data derived at the highest fields to be somewhat less reliable than those derived at lower fields.

The amount of angular misalignment required to explain the observed broadening of the transitions in large parallel fields is approximately $\pm 6°-8°$ for the TaS_2 intercalates and $\lesssim \pm 1.5°$ for the $TaS_{1.6}Se_{0.4}$ intercalates. These misoriented regions have also been seen[28] in single-crystal x-ray precession photographs of $TaS_2(pyridine)_{1/2}$. They may well be a property of the unintercalated metal, as discussed before. The buckling in TaS_2 appears to have a length scale of a fraction of a millimeter. For $NbSe_2$ and $TaS_{1.6}Se_{0.4}$, the much smaller misorientations may reflect the twinned growth of the crystals.

In order to check the validity of the procedures employed to determine H_{c2} further, we carried out some subsidiary measurements of the frequency dependence of the data, and also measurements of resistive transitions. Measurements of ac susceptibility were made at both 5 and 100 kHz. Values of $H_{c2\perp}$ so derived depend only slightly on the measuring frequency, and the values differ by less than the zero-field transition width. The frequency dependence of the results for $H_{c2\parallel}(T)$ is greater. This difference is no doubt related to the severe transition broadening observed for large parallel fields seen in Fig. 5. At low frequencies, a fully connected superconducting path is necessary for complete shielding, whereas at higher frequencies inductive effects allow partially connected superconducting regions to fully exclude the ac field. In light of the significant misorientations found in the TaS_2 crystals, the critical-field values derived at 100 kHz should represent more closely the values of H_{c2} for the regions with exactly parallel orientation. These values will therefore be used in the data presented in the next section.

Comparative measurements of resistive and ac susceptibility transitions were also made on a few samples. Resistive and ac susceptibility transitions for $TaS_2(pyridine)_{1/2}$ are shown in Fig. 6 for dc fields of zero and 3 kG. These are representative of the samples studied. The zero-field transitions are both relatively narrow. The ac susceptibility transition begins as the resistance goes to zero. This is the usual relationship between ac susceptible and resistive data. The broadening of the zero-field resistive transition above T_c (3.47 K) may be due to fluctuation effects, which are predicted to give an enhanced conductivity of roughly the observed magnitude. In a finite field, both transitions are broader but still roughly overlap. However, a new feature shows up in the resistive transition—a long, high-temperature "tail," extending to ~ 3.3 K, even though T_{c2} is ~ 2 K for a perpendicular field of 3 kG. It appears that this long tail is due to regions of the sample with higher critical temperatures which are substantially misoriented with respect to the overall sample orientation.

Support for this interpretation comes from data for resistive transitions for $NbSe_2$ in perpendicular dc fields. Here the end point of the high-temperature tail at the normal-state resistance corresponds quite closely to the temperature T_{c2} for the dc fields being oriented *parallel* to the layers. Similar admixing of the effects of misoriented regions has been noted previously for $NbSe_2$.[9] It is not clear why such badly misoriented regions occur in the $NbSe_2$ crystals, which appear visually to be of very high quality. In any case, discernible effects due to badly misoriented regions appear to be fairly common for these highly anisotropic superconductors. Still, the correspondence between the ac susceptibility and resistive tran-

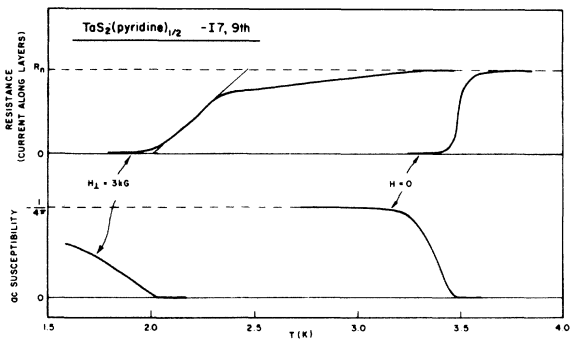

FIG. 6. Comparison of ac susceptibility and resistive transitions for perpendicular applied fields in $TaS_2(pyridine)_{1/2}$. Sensing currents flow in plane of layers in both cases. The high-temperature tail of the resistance transition in a 3-kG field appears to result from regions of the sample which are misoriented (see text).

sitions is satisfactory, once the origin of the long tail above $T_{c2}(H)$ is recognized.

Reproducibility of the critical-field data was found to be best within a given intercalation batch, typically 10 to 20% for $H_{c2\perp}$ and somewhat greater for $H_{c2\parallel}$. Different intercalation batches using crystals from the same parent powder demonstrated comparable reproducibility. The $TaS_2(\text{pyridine})_{1/2}$ sample were found to have the most reproducible properties, whereas $TaS_2(\text{collidine})_{1/6}$ was the least reproducible of the materials studied.

IV. CRITICAL-FIELD RESULTS

In this section we present data for the best samples of the intercalated compounds. Curves of $H_{c2}(T)$ for $TaS_2(\text{pyridine})_{1/2}$ are shown in Fig. 7 for various field orientations. In this figure the data for each field orientation have been scaled by a constant, and it is evident that the scaled curves coincide in the temperature range $1.6\ \text{K} < T < 3.2\ \text{K}$. Thus, in this range all curves have the same temperature dependence and a temperature-independent angular dependence, $H_{c2\theta}(T)/H_{c2\perp}(T)$ can be defined. The critical-field anisotropy $H_{c2\parallel}(T)/H_{c2\perp}(T)$ is seen to be 25. Very near T_c, however, the anisotropy decreases. Scaled curves of $H_{c2\theta}(T)$ for $TaS_2(\text{aniline})_{3/4}$ are shown in Fig. 8. In contrast to $TaS_2(\text{pyridine})_{1/2}$, here the data for the parallel orientation show a marked deviation from universal scaling. The data for $TaS_{1.6}Se_{0.4}(\text{collidine})_{1/6}$ are shown in Fig. 9 where once again we observe universal scaling.

Beyond doubt the most striking feature of the $H_{c2}(T)$ for all the intercalated compounds is how large the parallel critical fields are for these superconductors, despite their low transition temperatures. They are like no other bulk superconductors previously studied. The data in Figs. 7–9 are not plotted so as to dramatize this particular feature, but note that for all the intercalated samples the parallel critical fields at low temperatures exceed 100 kOe and were too large to measure. Not surprisingly, the critical fields for the unintercalated material $NbSe_2$ are not as large, but still substantial compared with conventional type-II superconductors. The perpendicular critical fields for all the intercalated compounds are by contrast quite low. Correspondingly, the anisotropies in H_{c2} are very large as indicated by the scaling factors shown on the figures and used in plotting the data.

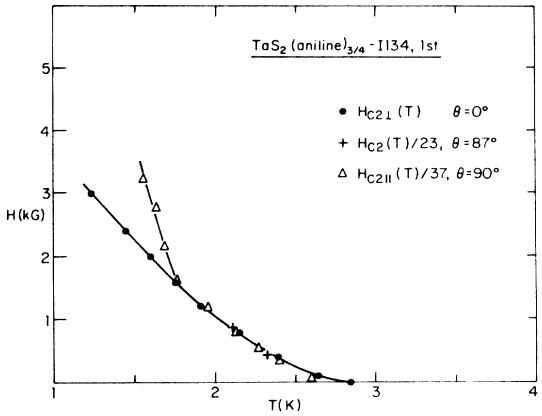

FIG. 8. Critical fields at various angles for $TaS_2(\text{aniline})_{3/4}$. Curves scaled as in Fig. 7. Note upward rise of $H_{c2\parallel}$ at low temperatures.

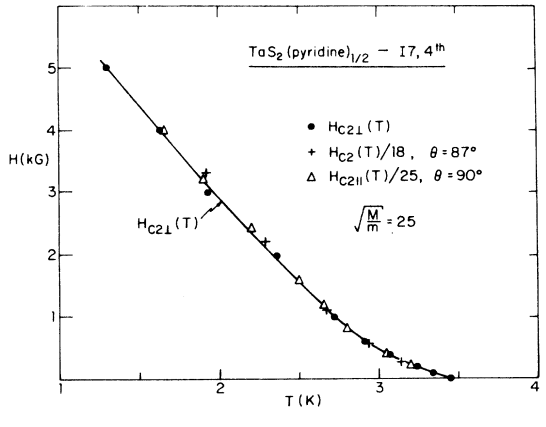

FIG. 7. Critical fields at various angles for $TaS_2(\text{pyridine})_{1/2}$. For each orientation the curves can be scaled to the perpendicular critical-field data. Scaling factors indicated.

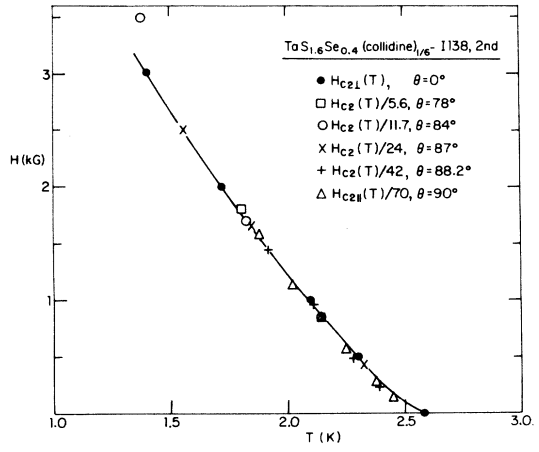

FIG. 9. Critical fields at various angles for $TaS_{1.6}Se_{0.4}(\text{collidine})_{1/6}$. Curves scaled as in Fig. 7. The angular dependence of H_{c2} is plotted in Fig. 10.

The data in Figs. 7–9 and the data for the other intercalated compounds also show that, despite the enormous anisotropy of these materials, to first order the critical fields for all angles can be scaled onto a single curve that depends only on temperature. For some of the materials this scaling breaks down slightly near T_c. But as we discuss later below, the observed behavior near T_c is peculiar in some ways, and may not reflect intrinsic behavior.

The one striking deviation from this apparent scaling behavior is the data for $TaS_2(aniline)_{3/4}$ in the parallel field direction (Fig. 8). Here at low tempertures $H_{c2\parallel}$ rises markedly upward from the scaled curve in a manner qualitatively like that predicted by the Josephson-coupled models discussed in Sec. II. A second sample of $TaS_2(aniline)_{3/4}$ studied showed a similar upturn, but unfortunately the data for this sample do not extend to as high fields. This deviation from scaling is perhaps not surprising, since this compound has the largest layer separation ($\delta = 12.1$ Å) of all the compounds studied. On the other hand, it is not as anisotropic as $TaS_{1.6}Se_{0.4}$ $(collidine)_{1/6}$ for which no upturn is evident. As we shall see later, however, these facts are not necessarily inconsistent.

Detailed measurements of the angular dependence of H_{c2} were carried out for $NbSe_2$, $TaS_{1.6}Se_{0.4}$, and $TaS_{1.6}Se_{0.4}(collidine)_{1/6}$. Results for the angular dependence of H_{c2} for $TaS_{1.6}Se_{0.4}(collidine)_{1/6}$ are shown in Fig. 10 along with the anisotropic GL prediction [Eq. (2)], which should be applicable at the temperatures used. The mass ratio is defined from Eq. (4). We see that the anisotropy is indeed very large, $(M/m)^{1/2} = 70$. Apparent deviations above the anisotropic GL prediction are evident near parallel. This is very likely due to the extrapolation procedure we have used to determine H_{c2}, which near parallel will tend to mix in contributions from regions of higher H_{c2} present that are due to misorientations ($\sim 1.5°$ appear present), thereby broadening the experimentally determined $H_{c2}(\theta)$ curve. For compounds with very large anisotropies, a precise determination of $H_{c2}(\theta)$ is thus clearly very difficult and such data must be treated with some caution. However, while it is difficult to extract the true value of $H_{c2}(\theta)$ for orientations near parallel, it is not as problematic for the exactly parallel orientation, as H_{c2} is a maximum for that orientation.

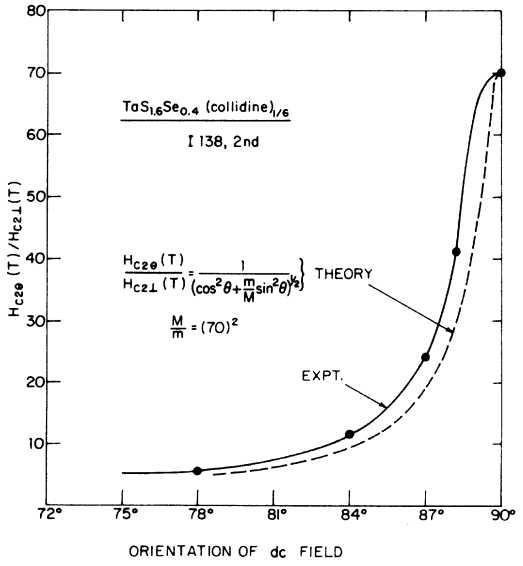

FIG. 10. Angular dependence of the critical fields of $TaS_{1.6}Se_{0.4}(collidine)_{1/6}$, and the prediction of the anisotropic GL theory, using Eq. (4) to determine (M/m). Only angles near parallel are shown.

For $NbSe_2$ and $TaS_{1.6}Se_{0.4}$ we find general accord between the experimental values and the anisotropic GL result. At intermediate angles, however, the experimental values fall slightly *below* those predicted theoretically. Similar deviations for $NbSe_2$ have been reported previously[8] and are presumably intrinsic.

An unusual feature of the critical-field behavior of all the materials studied is their failure to show a clearly defined linear dependence of H_{c2} with temperature as $T \to T_c$. On theoretical grounds such a linear dependence is expected sufficiently close to T_c in any bulk superconductor. In fact, to varying degrees the temperature dependence of the scaled critical fields for all compounds show a positive curvature in the neighborhood of T_c. There is absolutely no evidence in any of the materials for the $(T_c - T)^{1/2}$ temperature dependence of $H_{c2\parallel}$ that is the theoretically expected signature for fully decoupled (i.e., independent) layers. In addition to the curvature near T_c, at lower temperatures the observed critical fields increase with decreasing temperature faster than is typical of conventional type-II superconductors.[29] Positive curvature near T_c is least pronounced (but still present) for $NbSe_2$, which is the least anisotropic of the materials studied.

This positive curvature in H_{c2} near T_c has been noted previously[10] and is apparently a ubiquitous feature in all reported data. Similar curvature is also evident[30] in the critical-field curves of the quasi-one-dimensional superconductor $(SN)_x$. A much less dramatic positive curvature has been observed[31] in clean elemental type-II superconductors (Nb and V) well below T_c and has been explained as resulting from Fermi surface and gap anisotropy. In that case, however, H_{c2} was still linear in $(T_c - T)$ close to T_c. On the basis of our experimental results, it is impossible to determine if the curvature near T_c seen in our data is intrinsic. Our analysis in the following section will therefore concentrate on data for temperatures below the region of curvature very near T_c.

V. DISCUSSION

A. Determination of the superconducting material parameters

In order to establish the physical regimes (e.g., two or three dimensional, clean and dirty) in which the samples studied here belong, we use the results of the anisotropic GL theory described in Sec. II. In particular, using our data for $H_{c2}(T)$ and Eqs. (2) and (4), we can determine both the GL mass ratio M/m and the zero-temperature coherence lengths $\xi(0)$ and $\xi_z(0)$.

As a practical matter this involves using the critical field slopes dH_{c2}/dT at T_c to determine the desired parameters. However, because of the anomalous curvature in $H_{c2}(T)$ near T_c this procedure cannot be applied in a straightforward fashion. Consequently, in applying the GL results we have used the data in the region of linear (or at least nearly linear) temperature dependence of $H_{c2}(T)$ at lower temperatures. Under the circumstances this seems the only sensible choice. Of course the mass ratio is given directly by the scaling factor between $H_{c2\parallel}$ and $H_{c2\perp}$ independent of this curvature. A compilation of the mass ratios and coherence lengths so determined are given in Table II for all the compounds studied, along with the other important material parameters r and α that can be determined from them using Eqs. (10) and (11). In surveying the properties listed in Table II we find that the superconducting parameters of each group of intercalation compounds are rather similar. The T_c values are similar, as are the values of $dH_{c2\perp}/dT$. This is in accord with the model for the superconductivity of these compounds which starts with the picture of weakly coupled layers which have their own superconducting properties such as T_c and $\xi(0)$. The $dH_{c2\parallel}/dT$ values obtained for these compounds are all extremely large. Correspondingly the interlayer GL coherence lengths $\xi_z(0)$ are very small, in some cases less than the layer-to-layer spacing s. These small coherence lengths are also reflected in the small values of the interlayer coupling parameter ($r \lesssim 1$) indicating that these materials are candidates for exhibiting quasi-two-dimensional superconductivity. The unintercalated compounds included in the table are far less unusual and have larger interlayer coupling parameters ($r > 1$). Consequently they are expected to show three-dimensional-like behavior even at the lowest temperatures.

A somewhat surprising result for the TaS_2 intercalation complexes is that the values of $dH_{c2\parallel}/dT$ and the critical-field anisotropy, $H_{c2\parallel}(T)/H_{c2\perp}(T)$, are all rather similar, even though the separation between metallic layers increases from 3.6 Å for TaS_2 (collidine)$_{1/6}$ to 12.1 Å for TaS_2(aniline)$_{3/4}$. It is possible to understand this result in terms of a Josephson-tunneling mechanism for coupling, although a rather long tunneling length is required (see below). For the $TaS_{1.6}Se_{0.4}$ compounds the derived values of $\xi_z(0)$ are even shorter than for the TaS_2 compounds. Significantly, the anisotropies for both the intercalated compounds of $TaS_{1.6}Se_{0.4}$ are very much larger than for the unintercalated metal $TaS_{1.6}Se_{0.4}$. With this result there can be little doubt, if there was any, that the intercalation of organic molecules causes the large critical-field anisotropy observed for these compounds.

TABLE II. Critical-field and material parameters for the layered compounds.

	T_c (K)	$\frac{dH_{c2\perp}}{dT}$ (kG/K)	$\frac{dH_{c2\parallel}}{dT}$ (kG/K)	$\left(\frac{M}{m}\right)^{1/2}$	$\xi(0)$ (Å)	$\xi_z(0)$ (Å)	$r = \frac{4}{\pi}\left[\frac{\xi_z(0)}{s/2}\right]^2$	$\alpha = \frac{(dH_{c2\parallel}/dT)}{18.95\,\text{kG/k}}$
TaS_2(collidine)$_{1/6}$ $\delta = 3.6$ Å	3.2	3.3	~100	30	180	6.0	1.95	5.3
TaS_2(pyridine)$_{1/2}$ $\delta = 6.0$ Å	3.47	2.8	70	25	183	7.3	1.90	3.7
TaS_2(aniline)$_{3/4}$ $\delta = 12.1$ Å	2.9	2.6	96	37	209	5.6	0.50	5.1
$TaS_{1.6}Se_{0.4}$	4.1	8.0	44	5.5	100	18.2	4.53	2.32
$TaS_{1.6}Se_{0.4}$(collidine)$_{1/6}$ $\delta = 3.6$ Å	2.6	3.4	240	70	193	2.8	0.41	12.7
$TaS_{1.6}Se_{0.4}$(pyridine)$_{1/2}$ $\delta = 5.9$ Å	2.1	3.0	225	75	228	3.0	0.32	11.9
$NbSe_2$	7.1	8.0	23	2.9	76	26	87	1.23

Additional information about the material parameters of these compounds can be obtained if we assume that the intralayer behavior of these superconductors is approximately described by the conventional theory of type-II superconductivity.[29] We can relate $\xi(0)$ and the BCS coherence length ξ_0 to the normal-state properties of the material using the relationships[32]

$$\xi_0 = 7.95\times10^{-17}(n^{2/3}S/S_F)(\gamma T_c)^{-1} , \quad (13)$$

$$l = 1.27\times10^{4}[\rho(n^{2/3}S/S_F)]^{-1} , \quad (14)$$

$$\xi(0) = 0.74\xi_0[\chi(\xi_0/l)]^{1/2} , \quad (15a)$$

$$= \begin{cases} 0.74\xi_0, & l \gg \xi_0 , \quad (15b) \\ 0.85(\xi_0 l)^{1/2} = 8.6\times10^{-7}(\rho\gamma T_c)^{-1/2}, & l \ll \xi_0 , \quad (15c) \end{cases}$$

where l is the electron mean free path, n is the electron density (in cm^{-3}), γ the linear (electronic) coefficient of the specific heat (in $\mathrm{erg/cm^3\,K^2}$), ρ is the normal-state resistivity (in Ω cm), χ is the well-known Gor'kov function,[20] and S/S_F is a weighting factor to account for the actual area of the Fermi surface as compared with a free-electron Fermi surface.

In principle, then, knowledge of the normal-state parameters n, S/S_F, γ, ρ, and T_c permits the determination of ξ_0, l, and $\xi(0)$. Since the product $n^{2/3}S/S_F$ is not known for the layered compounds, we can instead use the measured values of γ, ρ, $\xi(0)$, and T_c to determine ξ_0, l, and $n^{2/3}S/S_F$. If the values of $n^{2/3}S/S_F$ inferred in this way are physically reasonable, we conclude that the observed $\xi(0)$'s are consistent with the measured normal-state parameters and the conventional theory. In addition this procedure allows us to estimate whether the intralayer behavior is in the clean or dirty limit.

The results of this analysis are shown in Table III for the materials where measurements of ρ and γ are available. For the unintercalated compounds $NbSe_2$ and $TaS_{1.6}Se_{0.4}$ this procedure leads to the parameters shown in Table III. For the intercalated compounds $TaS_2(\text{pyridine})_{1/2}$ and $TaS_{1.6}Se_{0.4}(\text{pyridine})_{1/2}$, however, a self-consistent set of parameters cannot be obtained. This is because the coherence lengths calculated using even Eq. (15c) are smaller than the measured values. [$\xi(0)_{\text{calc}} = 156$ and 94 Å, respectively, for these two materials.] Note that since the dirty limit [Eq. (15c)] appears to apply for these materials, this disagreement and the resultant failure to obtain self-consistency is independent of our lack of values for $n^{2/3}S/S_F$. Because of this problem the entries in Table III for the intercalated samples were calculated assuming the indicated values of $n^{2/3}S/S_F$, which were obtained by assuming $S/S_F = 1$ and one conduction electron per molar volume. (A similar assumption for $NbSe_2$ and $TaS_{1.6}Se_{0.4}$ gives values of $n^{2/3}S/S_F$ within 30% and 10%, respectively, of the values inferred from the data and listed in Table III, thus providing some justification for this procedure.)

Also shown in the table for use later in comparisons with microscopic theory are estimated minimum values of the normalized spin-orbit scattering time $\tau_{so}T_c$ [see Eq. (12)] using the values of l and ξ_0 in Table III

$$\tau_{so}T_c^{(\min)} \equiv 2l/3\pi(1.17\xi_0) . \quad (16)$$

We expect this to be a minimum value because the total scattering rate must be larger than (or equal to) the rate for spin-orbit scattering, so that the mean free path l is always less than or equal to l_{so}; i.e., $l \leq l_{so}$.

We conclude from this discussion and from Tables

TABLE III. Additional material parameters for the layered compounds. Parentheses indicate parameters are not completely self-consistent. See text.

	$\xi(0)$ Expt. (Å)	$\rho_{\parallel}$ (Ω cm)	γ (mJ mole^{-1} K^{-2})	ξ_0 (Å)	l (Å)	ξ_0/l	$n^{2/3}S/S_F$ (cm^{-2})	$\tau_{so}/T_c^{(\min)}$ theory	$\tau_{so}T_c$ Expt.
$NbSe_2$	82[a]	3.5×10^{-6} [a]	16.5[b]	120	810	0.15	6.2×10^{14}	1.12	Not determined
$TaS_{1.6}Se_{0.4}$	100[c]	4.5×10^{-5} [d]	11.2[b]	350	49	7.2	5.8×10^{14}	0.025	Not determined
$TaS_2(\text{pyridine})_{1/2}$	180[c]	5.7×10^{-5} [e]	9.1[b]	(740)	(53)	(14)	(4.2×10^{14})	0.013	0.01
$TaS_{1.6}Se_{0.4}(\text{pyridine})_{1/2}$	230[c]	2.9×10^{-4} [d]	9.3[b]	(1200)	(10)	(120)	(4.2×10^{14})	0.0016	0.01

[a] P. Garoche, J. J. Veyssié, P. Manuel, and P. Molinié, Solid State Commun. 19, 455 (1976). In this study of $NbSe_2$ both $H_{c2\perp}$ and resistivity were measured.

[b] Reference 13. Lattice constants of layered compounds are given in Refs. 22 and 24.

[c] From this work, Table II.

[d] Reference 24.

[e] A. Thompson, F. Gamble, and B. Koehler, Phys. Rev. B 5, 2811 (1972).

II and III that the intercalated compounds are in the dirty limit ($l < \xi_0$), and that the limits for which KBL obtained results are appropriate for these compounds. The unintercalated metal $NbSe_2$ is, in contrast, a relatively clean superconductor, and fully in the three-dimensional limit.

B. Comparison with microscopic theory

In this section we compare our experimental results with microscopic theory, specifically the predictions of the KBL theory. Since the most interesting physical effects are expected to manifest themselves in the parallel field orientation, we focus our discussion on those data.

A comparison of the KBL theoretical predictions with experiment for $H_{c2\parallel}(T)$ are shown in Figs. 11–13 for $TaS_2(\text{pyridine})_{1/2}$, $TaS_2(\text{aniline})_{3/4}$, and $TaS_{1.6}Se_{0.4}(\text{collidine})_{1/6}$. (Note that experimental data on additional samples not shown earlier are included in these figures for completeness.) The theoretical curves were generated by means of a computer program which used simple analytical functions to approximate the results obtained by KBL. Material parameters for each compound, r and α, are taken from Table II, and T_c values for this fitting procedure only are determined from fitting the linear portion of the $H_{c2\parallel}(T)$ curves. The normalized spin-orbit scattering time, $\tau_{so}T_c$, is treated as an adjustable parameter.

For the $TaS_2(\text{pyridine})_{1/2}$ samples only a fair fit can be achieved with the theoretical curves, although reasonable agreement is seen for one of the samples.

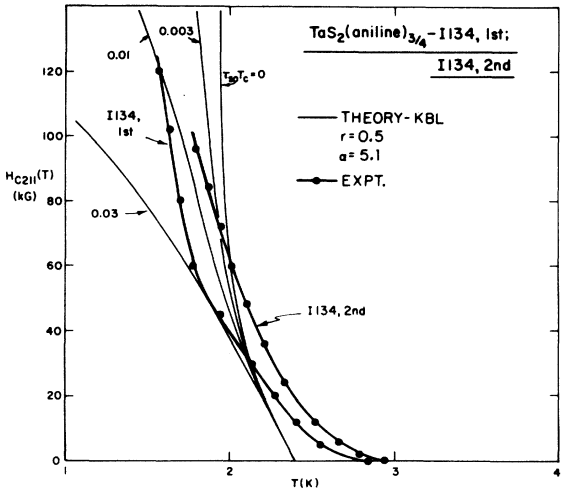

FIG. 12. Comparison of parallel critical fields of $TaS_2(\text{aniline})_{3/4}$ with predictions of KBL theory for various values of $\tau_{so}T_c$. Material parameters α and r from Table II.

The curve for *I*7–5th (the fifth intercalation run from batch *I*7 of reacted TaS_2) shows some indication of an upturn, while the curve for *I*7–4th rises more slowly. These uncertainties in the measured critical field curves were discussed earlier and certainly reflect the problem of extracting correct values of $H_{c2\parallel}(T)$ from severely broadened transitions. Still, the overall fit at intermediate temperatures is best for both samples using $\tau_{so}T_c \simeq 0.01$. Based on this fitting procedure, a value of 0.01 is listed in Table III as

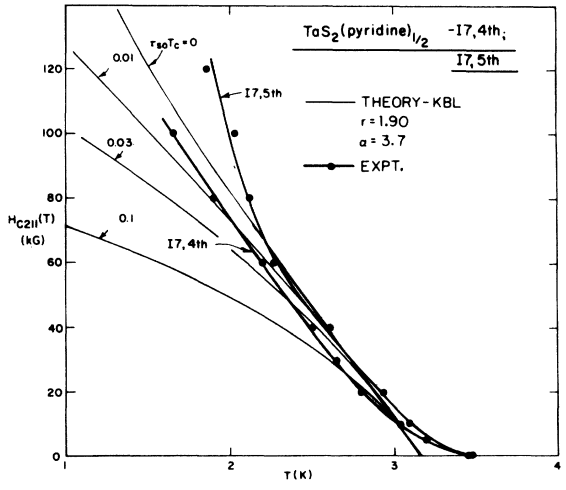

FIG. 11. Comparison of parallel critical fields of $TaS_2(\text{pyridine})_{1/2}$ with predictions of KBL theory for various values of $\tau_{so}T_c$. Material parameters α and r taken from Table II. For the theoretical curves only, T_c is determined by extrapolating the perpendicular field curve to zero field.

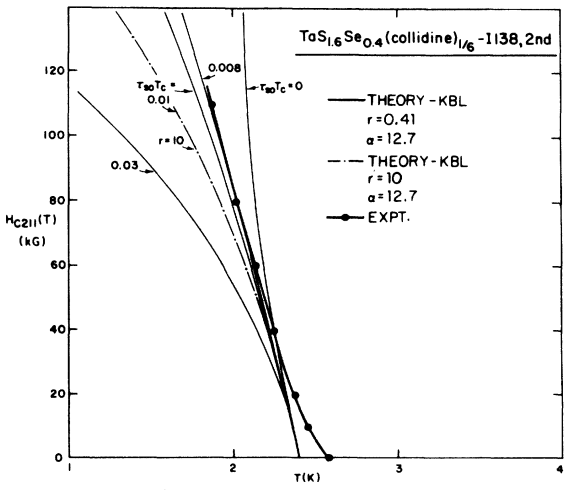

FIG. 13. Comparison of parallel critical fields of $TaS_{1.6}Se_{0.4}(\text{collidine})_{1/6}$ with predictions of KBL theory for various values of $\tau_{so}T_c$. Curve for $r = 10$ indicates the prediction for well coupled layers (i.e., three-dimensional-like behavior). Material parameters taken from Table II.

the experimentally determined value of $\tau_{so}T_c$.

The experimental curves for $TaS_2(aniline)_{3/4}$ shown in Fig. 12 can also be fitted approximately by the theory, again with $\tau_{so}T_c \simeq 0.01$. The sharp upturn at low temperatures for *I*134–1st, and *I*134–2nd, is probably significant, as both experimental curves show this upturn. Also, for $TaS_2(aniline)_{3/4}$ the material parameters are such that an upturn of $H_{c2\parallel}(T)$ is definitely expected, even for the apparently canonical $\tau_{so}T_c \simeq 0.01$. These data then qualitatively demonstrate the effects of the decoupling of the layers when $\xi_z(T) < s/\sqrt{2}$. Theoretical fitting to the critical-field curve for $TaS_2(collidine)_{1/6}$, not shown, is less successful, though the best fit is still for $\tau_{so}T_c \simeq 0.01$. This $TaS_2(collidine)_{1/6}$ crystal looks, under inspection in an optical microscope, to be the poorest quality, most wrinkled sample.

The fit between theory and experiment for the intercalated compounds of $TaS_{1.6}Se_{0.4}$ have been carried out in a similar fashion. Here again the best fit is obtained for $\tau_{so}T_c \simeq 0.01$ as seen for the case illustrated [$TaS_{1.6}Se_{0.4}(collidine)_{1/6}$] in Fig. 13. The theoretical curve for a well-coupled system ($r = 10$) is also shown for comparison. The quality of the fit is somewhat better than that in Figs. 11 and 12, neglecting again the curvature near T_c. Note that for both $TaS_{1.6}Se_{0.4}$ compounds, the temperature range covered includes the temperature T^* at which the metallic layers are expected to "decouple." However, there is no evidence of an upturn in the experimental data. This can be understood from the theoretical curves of Ref. 6 for various values of $\tau_{so}T_c$. We see that upward curvature is expected to manifest itself only for very much shorter spin-orbit scattering times. Therefore, the absence of an upturn in the experimental data does not imply that the layers have not decoupled.

The fit to the data exhibited in Figs. 11 to 13 is semiquantitative at best. Given the problems with the data and the simplicity of the theoretical model, this is perhaps all one can expect. A more interesting and perhaps compelling aspect of the agreement between theory and experiment is that the theory provides a very nice account of the observed *systematics* in the data, specifically which samples should show the upturn in $H_{c2\parallel}$ at low temperatures and which should not. This point is illustrated in Fig. 14 where we have summarized the data by plotting normalized experimental and theoretical critical-field curves for $TaS_2(pyridine)_{1/2}$, $TaS_2(aniline)_{3/4}$, and $TaS_{1.6}Se_{0.4}(collidine)_{1/6}$, for the single best-fit value of $\tau_{so}T_c = 0.01$. Results are shown only for the best samples. Comparing the group of experimental curves with the group of theoretical curves, we find that, considering all the problems encountered in measuring $H_{c2\parallel}(T)$, the KBL results provide a fairly good account of the systematic trends in the data. We regard this as at least a tentative confirmation of the KBL theory.

An interesting aspect of the above theoretical fits is that in each case the best fit corresponds to $\tau_{so}T_c \simeq 0.01$. This is in accord with the general idea that the properties of the individual layers in the intercalated materials, being two-dimensional-like, are relatively insensitive to the exact intercalation species. The values of the spin-orbit scattering times required

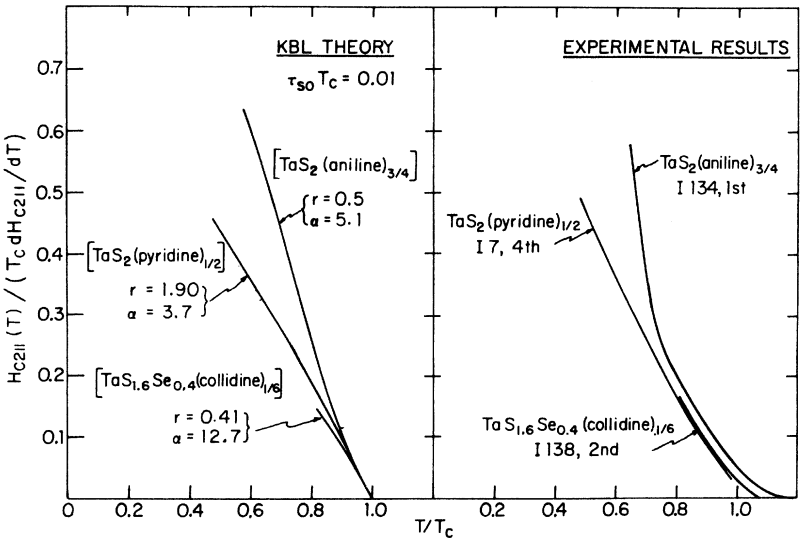

FIG. 14. Comparison of systematic trends in parallel critical fields observed in intercalated compounds with predictions of KBL theory using best-fit value of $\tau_{so}T_c = 0.01$. Parameters α and r as before are taken from Table II. Experimental curves are shown with temperature normalization from fitting perpendicular-critical-field data.

are, however, very short ($\tau_{so} \simeq 2 \times 10^{-14}$ sec) and the question arises whether such short scattering times are physically reasonable. Lacking any *a priori* knowledge of τ_{so}, we can only insist that the spin-orbit scattering rate τ_{so}^{-1} not exceed the total scattering rate τ^{-1}. Thus the total electron-scattering lifetime τ can be used to put a lower limit on τ_{so} and estimates of $\tau_{so} T_c^{(\min)} \equiv \tau T_c$ are given in Table III. Based on the estimated value of $\tau_{so} T_c^{(\min)}$ obtained for TaS_2(pyridine)$_{1/2}$, we see that the spin-orbit scattering rate required to fit the data is comparable to this maximum physically allowed rate. Since the spin-orbit scattering rate is usually significantly less than the total scattering rate,[20] our results suggest that additional mechanisms for reducing Pauli limiting in the dirty limit are operative in these layered materials. Some new mechanisms for reducing Pauli limiting in layered compounds have recently been proposed,[33] but all appear to be applicable only in clean materials.

An alternative possibility is that electron-phonon strong coupling effects may partly reduce the effects of Pauli paramagnetic limiting, so that the proper inclusion of strong-coupling effects in the theory would lead to larger, and more acceptable experimental values for τ_{so}. Recently this has been shown[32] to be the case for Nb_3Sn. None of the present theories for layered or strongly anisotropic superconductors has incorporated these strong-coupling effects explicitly, however. This is clearly a question which deserves further theoretical and experimental study.

C. Dependence of the interlayer coupling on layer separation

In the Josephson-coupled model of the superconducting layered compounds (or in the tight-binding approximation to which it can be related), the interlayer coupling parameter η is expected to fall off exponentially with layer separation δ [$\eta = \eta_0 \times \exp(-\delta/\delta_0)$], all else being equal—that is, if we assume for any given intercalation series the characteristic tunneling length δ_0 is independent of the particular intercalation species. Using Eqs. (1), (3), and (11) and the fact that $\xi(0)$ is nearly independent of intercalation species, we have

$$\eta = \frac{\hbar^2}{2s^2 M} = \frac{\hbar^2}{2s^2 m}\left[\frac{\xi_z(0)}{\xi(0)}\right]^2 \propto r \quad . \tag{17}$$

Thus we can use the dependence of r or δ to estimate δ_0.

From Table II we see that the values of r for TaS_2(collidine)$_{1/6}$ and TaS_2(pyridine)$_{1/2}$ are roughly equal while the value for TaS_2(aniline)$_{3/4}$ is substantially smaller even though in this series δ progresses from $\delta = 3.6$ to 6.0 to 12.1 Å. The data for TaS_2(collidine)$_{1/6}$ and TaS_2(pyridine)$_{1/2}$ are not consistent with an exponential decrease of η with δ, and since the data for TaS_2(collidine)$_{1/6}$ appear to be less reliable than that for the other compounds, we exclude them from this analysis. Assuming an exponential dependence for η, the data for TaS_2(pyridine)$_{1/2}$ and TaS_2(aniline)$_{3/4}$ yield a value of $\delta_0 = 4.6$ Å. Comparison of the two $TaS_{1.6}Se_{0.4}$ intercalates yields $\delta_0 = 9.3$ Å. These tunneling lengths are large compared to those typical of oxide-layer tunnel junctions ($\delta_0 \simeq 1.5$ Å) but perhaps not unreasonable for organic molecules. We have not investigated the electronic structure of these molecules to estimate what the height of tunneling barrier is likely to be. Finally, we should point out that we do not rule out the possibility that microshorts between layers might be contributing to the interlayer coupling. If such shorts were dense on the scale of the in-plane GL coherence length $\xi(T)$, the Josephson model used to analyze the data should still apply, but then an exponential dependence of η on δ would not be expected.

VI. SUMMARY AND CONCLUSIONS

In this paper we have presented measurements of the upper critical fields of a series of intercalated layered superconductors, and of two unintercalated compounds. We find that the intercalated compounds should behave two dimensionally at low temperatures, while the behavior near T_c is three dimensional in character. Furthermore, for the intercalated compounds, the layers themselves are in the dirty limit ($l \ll \xi_0$). In contrast, unintercalated $NbSe_2$ is a relatively clean, three-dimensional (though anisotropic) superconductor.

To investigate the dimensional-crossover effect in the intercalated compounds, extensive comparisons were made between the experimental data and the microscopic theory of Klemm, Beasley, and Luther, which is based on the Josephson-coupled two-dimensional superconductor model. These comparisons show semiquantitative agreement between theory and experiment, allowing for the known difficulties with the parallel-field data. Evidence for the crossover to two-dimensional behavior at low temperatures is seen most clearly in the data for TaS_2(aniline)$_{3/4}$. Further support for the theoretical model is seen in the overall comparisons between theory and experiment, shown in Fig. 14, where the systematics of the theoretical predictions match well the experimental trends.

An unresolved question raised by the analysis is the origin of the very short spin-orbit scattering times required. These times appear to be at the lower limit of that possible for random spin-orbit scattering. Additional mechanisms for reducing Pauli limiting of H_{c2} thus appear to be required to account for the critical-field data. Resolution of this and other questions will require further experiments, and likely

better quality samples.

This study, therefore, in combination with our previous study of the fluctuation-induced diamagnetism of layered superconductors, provides substantial evidence confirming the essential predictions of the Josephson-coupled two-dimensional superconductor model. The quasi-two-dimensional nature of these compounds is seen to lead to their novel superconducting properties.

The effects of reduced dimensionality may also be important in other superconducting compounds, such as the filamentary (quasi-one-dimensional) compounds $(SN)_x$,[30] and the Chevrel compounds,[34] of which $PbMo_6S_8$ is an example. These latter compounds have been described as zero-dimensional units coupled in three dimensions.[34] It appears, however, that while the notion of reduced dimensionality may be relevant to understanding the large critical fields of these other compounds, the interunit coupling is not sufficiently weak for dimensional-crossover effects to be evident. In this respect, the intercalated layered compounds differ and appear to be unique. The intercalated compounds thus serve as model superconducting systems of reduced dimensionality.

ACKNOWLEDGMENTS

We wish to thank R. A. Klemm, A. Luther, M. Tinkham, and T. H. Geballe for helpful discussions throughout the course of this work and A. H. Thompson for providing some of the samples. We also would like to thank S. Ruggiero for carrying out the computations for Table III, and B. J. Dalrymple for measurements further testing our procedures of data analysis. The experimental aspects of this work were carried out at Harvard University with the support and interest of Professor M. Tinkham. We are also grateful to the NSF and the Schlumberger Foundation for the support of the work one of us (D.E.P.) during the course of the experiments at Harvard. This research was supported by NSF Grants No. DMR 76-09591 (Yale) No. DMR 75-04368 (Stanford), and No. DMR 72-03060 (Harvard). Samples were prepared under support of AFOSR.

---

*Present address: Intermagnetics General Corp., Guilderland, N.Y. 12084.

[1]F. R. Gamble, F. J. DiSalvo, R. A. Klemm, and T. H. Geballe, Science 168, 568 (1970); F. R. Gamble, J. H. Osiecki, M. Cais, R. Pisharody, F. J. DiSalvo, and T. H. Geballe, *ibid.* 174, 493 (1971).

[2]Preliminary reports of this work have been given by D. E. Prober, M. R. Beasley, and R. E. Schwall, Bull. Am. Phys. Soc. 20, 342 (1975); D. E. Prober, Ph.D. thesis (Harvard University, 1975) (unpublished), available as Technical Report No. 10 (Tinkham Series), Division of Applied Sciences, Harvard University.

[3]L. N. Bulaevskii, Usp. Fiz. Nauk 116, 449 (1975) [Sov. Phys.-Usp. 18, 514 (1976)].

[4]D. W. Murphy, F. J. DiSalvo, G. W. Hull, Jr., J. V. Waszczak, S. F. Meyer, G. R. Stewart, S. Early, J. V. Acrivos, and T. H. Geballe, J. Chem. Phys. 62, 967 (1975).

[5]D. E. Prober, M. R. Beasley, and R. E. Schwall, Phys. Rev. B 15, 5245 (1977).

[6]R. A. Klemm, M. R. Beasley, and A. Luther, J. Low Temp. Phys. 16, 607 (1974); R. A. Klemm, A. Luther, and M. R. Beasley, Phys. Rev. B 12, 877 (1975).

[7]W. E. Lawrence and S. Doniach, in *Proceedings of the Twelfth International Conference on Low-Temperature Physics,* edited by E. Kanda (Academic Press of Japan, Kyoto, 1971), p. 361.

[8]See, for example, R. C. Morris, R. V. Coleman, and Rajendra Bhandari, Phys. Rev. B 5, 895 (1972); P. de Trey, Suso Gygax, and J. -P. Jan, J. Low Temp. Phys. 11, 421 (1973); and S. Foner and E. J. McNiff, Jr., Phys. Lett. A 45, 492 (1973).

[9]H. A. Leupold, F. Rothwarf, J. J. Winter, J. T. Breslin, R. L. Ross, T. R. AuCoin, and L. W. Dubeck, J. Appl. Phys. 45, 5399 (1974).

[10]John A. Woollam and Robert B. Somoano, Phys. Rev. B 13, 3843 (1976).

[11]S. Foner, E. J. McNiff, Jr., A. H. Thompson, F. R. Gamble, T. H. Geballe, and F. J. DiSalvo, Bull. Am. Phys. Soc. 17, 289 (1972); also S. Foner (private communication).

[12]R. C. Morris and R. V. Coleman, Phys. Rev. B 7, 991 (1973).

[13]R. E. Schwall, G. R. Stewart, and T. H. Geballe, J. Low Temp. Phys. 22, 557 (1976).

[14]Y. Muto, Y. Okada, N. Kobayashi, N. Toyota, and M. Ikebe, J. Phys. (Paris) 39, C6-458 (1978).

[15]B. S. Chandrasekhar, Appl. Phys. Lett. 1, 7 (1962); A. M. Clogston, Phys. Rev. Lett. 3, 266 (1962). For a modern review see K. Maki, in *Superconductivity,* edited by R. Parks (Marcel Dekker, New York, 1969), Chap. 18, also, references therein.

[16]D. R. Tilley, Proc. Phys. Soc. London 86, 289, 678 (1965); also E. I. Kats, Zh. Eksp. Teor. Fiz. 56, 1675 (1969) [Sov. Phys.-JETP 29, 897 (1969)].

[17]L. N. Bulaevskii, Zh. Eksp. Teor. Fiz. 64, 2241 (1973) [Sov. Phys.-JETP 37, 1133 (1973)]; and N. Boccara, J. P. Carton, and G. Sarma, Phys. Lett. A 49, 165 (1974).

[18]K. Takanaka, Phys. Status Solidi B 68, 623 (1975); and H. W. Pohl and H. Teichler, *ibid.* 75, 205 (1976).

[19]L. N. Bulaevskii, Zh. Eksp. Teor. Fiz. 65, 1278 (1973) [Sov. Phys.-JETP 38, 634 (1974)]; also L. N. Bulaevskii and A. A. Guseinov, Pis'ma Zh. Eksp. Teor. Fiz. 19, 742 (1974) [JETP Lett. 19, 382 (1974)].

[20]For general reviews of the theory of type-II superconductors from the point of view of the GL theory and its extensions see A. L. Fetter and P. C. Hohenberg, in *Superconductivity,* edited by R. Parks (Marcel Dekker, New York, 1969), Chap. 14; and N. R. Werthamer, *ibid.*, Chap. 6.

[21]F. R. Gamble, J. H. Osiecki, and F. J. DiSalvo, J. Chem. Phys. 55, 3525 (1971); and F. J. DiSalvo, Jr., Ph.D. thesis (Stanford University, 1971) (unpublished).
[22]J. A. Benda, R. E. Howard, and W. A. Phillips, J. Phys. Chem. Solids 35, 937 (1974).
[23]S. F. Meyer, R. E. Howard, G. R. Stewart, J. V. Acrivos, and T. H. Geballe, J. Chem. Phys. 62, 4411 (1975).
[24]J. F. Revelli, Jr., and W. A. Philips, J. Solid State Chem. 9, 176 (1974).
[25]A. H. Thompson, Nature (London) 251, 492 (1974).
[26]L. G. Rubin and W. N. Lawless, Rev. Sci. Instrum. 42, 571 (1971); W. N. Lawless, *ibid.* 46, 625 (1975).
[27]D. E. Prober, Rev. Sci. Instrum. 50, 387 (1979).
[28]R. R. Chianelli (private communication).
[29]Throughout this paper, by conventional type-II superconductors we mean those with isotropic, free-electron-like Fermi surfaces in the weak coupling limit. See Ref. 20.
[30]L. J. Azevedo, W. G. Clark, G. Deutscher, R. L. Greene, G. B. Street, and L. J. Suter, Solid State Commun. 19, 197 (1976).
[31]S. J. Williamson, Phys. Rev. B 2, 3545 (1970).
[32]T. P. Orlando, E. J. McNiff, Jr., S. Foner, and M. R. Beasley, Phys. Rev. B 19, 4545 (1979).
[33]Koya Aoi, Wolfgang Dieterich, and Peter Fulde, Z. Phys. 267, 223 (1974); K. B. Efetov and A. I. Larkin, Zh. Eksp. Teor. Fiz. 68, 155 (1975) [Sov. Phys.-JETP 41, 76 (1975)]; L. N. Bulaevskii and A. I. Rusinova, Pis'ma Zh. Eksp. Teor. Fiz. 21, 147 (1975) [JETP Lett. 21, 66 (1975)].
[34]D. Fisher, in *Proceedings of the Fourteenth International Conference on Low-Temperature Physics,* edited by Matti Krusius and Matti Vuorio (American Elsevier, New York, 1976), Vol. 5, p. 172. Granular aluminum films have also been described as zero-dimensional units coupled in three dimensions, although the strength of coupling depends on the methods of preparation.